

A simple method for seniority-zero quantum state preparation

Michał Krompiec,* Josh J. M. Kirsopp, Antonio Márquez Romero, and Vicente P. Soloviev

Fujitsu Research of Europe Ltd., Slough SL1 2BE, UK

E-mail: michal.krompiec@fujitsu.com

Abstract

Quantum Phase Estimation (QPE), the quantum algorithm for estimating eigenvalues of a given Hermitian matrix and preparing its eigenvectors, is considered the most promising approach to finding the ground states and their energies of electronic systems using a quantum computer. It requires, however, to be warm-started from an initial state with sufficiently high overlap with the ground state. For strongly-correlated states, where QPE is expected to have advantage over classical methods, preparation of such initial states requires deep quantum circuits and/or expensive hybrid quantum-classical optimization. It is well-known that orbital-optimized paired Coupled Cluster Doubles (oo-pCCD) method can describe the static correlation features of many strongly correlated singlet states. We show that pCCD and its unitary counterpart, UpCCD, become equivalent in the limit of small amplitudes if the amplitude matrix is sufficiently sparse. We demonstrate that substituting leading oo-pCCD amplitudes into the UpCCD Ansatz allows to prepare high-fidelity singlet states for models of multiple-bond dissociation in ethene, ethyne and dinitrogen, as well as for 1D Hubbard models at half-filling, with very shallow circuits. We envisage our method

to be of general use for approximate preparation of singlet states for Quantum Phase Estimation and related algorithms.

Introduction

Quantum Phase Estimation (QPE)^{1,2} is widely regarded as one of the most promising proposals for finding eigenvalues and eigenvectors of a given Hamiltonian using a quantum computer, particularly in cases where classical computing methods become computationally prohibitive. However, successful execution of QPE crucially depends on the value of the overlap of the *initial state* it acts upon with the target state being large enough.³ While a trivial initial state, e.g. the Hartree-Fock wavefunction, may often have a high overlap with the ground state of closed-shell molecules at their equilibrium geometries (see e.g. the G1 test set⁴), this is clearly not the case for strongly-correlated or ‘multi-reference’ systems. For these, several authors^{4–6} suggest performing an approximate Full Configuration Interaction (Full CI) calculation (such as Adaptive Sampling CI, ASCI,⁷ Stochastic Heat-bath CI, SHCI⁸ or CI Perturbatively Selected Iteratively, CIPSI⁹) on a classical computer and then encoding the CI state in a quantum circuit, using e.g. QROM¹⁰ or a specialized method for sparse states, such as CVO-QRAM.¹¹ It was also proposed^{6,12} to start with a Density Matrix Renormalization Group (DMRG)¹³ calculation and use Matrix Product State (MPS) circuit synthesis.^{12,14} While these methods are robust and versatile, they require rather deep quantum circuits, due to the heavy use of multi-controlled rotation gates. On the other hand, variational methods based on the Variational Quantum Eigensolver (VQE)¹⁵ can be used to construct shallower circuits: even the Efficient Symmetry Ansatz (which can parameterize any quantum state)¹⁶ results in about an order of magnitude lower number of quantum gates than CIPSI with CVO-QRAM, for hydrogen chains up to H_{14} .⁵ An adaptive method for Unitary Coupled Cluster ansatz construction can deliver even larger savings: Overlap-ADAPT-VQE yielded the same state fidelity for H_{14} as CIPSI/CVO-QRAM at

10^3 lower gate cost.⁵ It must be stressed, however, that VQE-based methods represent a challenging optimization problem,^{17,18} and suffer from prohibitive scaling of sampling cost with system size when executed on actual quantum computers.¹⁹ In this work, we introduce oo-pCCD-UpCCD, a low-cost state preparation method for singlet electronic states, yielding high-fidelity states without the need for variational optimization or deep circuits. We demonstrate the utility of our approach for determination of ground state energy of stretched ethene molecule using Quantum Phase Estimation.

Theory

Seniority-zero methods for singlet states

Let us consider the special case of strongly-correlated (or ‘multi-configurational’) singlet states. It is well-known that Doubly Occupied Configuration Interaction (DOCI, seniority-zero CI), defined as a linear combination of Slater determinants in which every spatial orbital is either unoccupied or doubly occupied, yields (when used with self-consistently optimized orbitals) an excellent description of static correlation in strongly-correlated systems with a spin of zero.^{20–23} Orbital-optimized paired Coupled Cluster Doubles (oo-pCCD) theory provides an inexpensive ($\mathcal{O}(N^2)$ amplitudes, $\mathcal{O}(N^3)$ time complexity of pCCD) yet surprisingly accurate approximation to DOCI especially for molecular Hamiltonians,²⁴ e.g. for dissociation of $\text{H}_4 - \text{H}_8$,^{20,24} dissociation of LiH, H_2O and N_2 ²⁴ as well as the 1-D²⁵ and 2-D Hubbard models.²⁶ Thus, pCCD appears to be an attractive starting point for designing a compact representation for singlet initial states.

Coupled Cluster methods in Quantum Circuits

Standard Coupled Cluster theories do not lend themselves to a direct representation in the form of a quantum circuit, because the exponentiated cluster operator $e^{\hat{T}}$ is non-unitary, where \hat{T} is a general excitations operator. On the other hand, Unitary Coupled Cluster

(UCC), which uses a unitary $e^{\hat{T}-\hat{T}^\dagger}$ operator instead, when truncated (e.g. at single and double excitations, as UCCSD) and approximated with a product formula forms a popular family of parameterized circuits used in VQE.²⁷ Quantum circuits implementing Unitary pCCD (UpCCD) have been introduced by Elfving et al. in the context of a ‘bosonic’ mapping^{28,29} and generalized to Jordan-Wigner mapping by Nam et al.³⁰ Thanks to the fact that paired double excitations obey bosonic statistics, there is no need to track state parity when transforming to the qubit basis, and each $e^{\hat{T}_a^i - \hat{T}_a^{i\dagger}}$ term is implemented by a Givens rotation, followed by a layer of CX gates,³⁰ in stark contrast to up to 8 *Pauli gadgets* (each consisting of a double CX ladder sandwiching a parameterized rotation) required for standard UCCD.³¹

Exact relations between CC, disentangled UCC and CI

The relation between trotterized (‘disentangled’) UCCSD, traditional CCSD and CI has been derived by Evangelista³² for the simple case of two electrons in four spinorbitals: $|\psi\rangle = c_1|1100\rangle + c_2|0110\rangle + c_3|1001\rangle + c_4|0011\rangle$. While the relation to CCSD is simple:

$$\Psi_{CCSD} = e^{t_1 \hat{a}_2^\dagger \hat{a}_0 + t'_1 \hat{a}_3^\dagger \hat{a}_1 + t_2 \hat{a}_2^\dagger \hat{a}_3^\dagger \hat{a}_1 \hat{a}_0} |1100\rangle \quad (1)$$

$$c_1 = 1, c_2 = t_1, c_3 = t'_1, c_4 = t_2 + t_1 t'_1, \quad (2)$$

the CI coefficients corresponding to one choice of operator ordering in disentangled UCCSD are:³²

$$\Psi_{UCCSD} = e^{t'_1 (\hat{a}_3^\dagger \hat{a}_1 - \hat{a}_1^\dagger \hat{a}_3)} e^{t_2 (\hat{a}_2^\dagger \hat{a}_3^\dagger \hat{a}_1 \hat{a}_0 - \hat{a}_0^\dagger \hat{a}_1^\dagger \hat{a}_3 \hat{a}_2)} e^{t_1 (\hat{a}_2^\dagger \hat{a}_0 - \hat{a}_0^\dagger \hat{a}_2)} |1100\rangle \quad (3)$$

$$\begin{aligned} c_1 &= \cos(t_1) \cos(t'_1) \cos(t_2) \\ c_2 &= \sin(t_1) \cos(t'_1) \cos(t_1) \sin(t'_1) \sin(t_2) \\ c_3 &= \cos(t_1) \sin(t'_1) \cos(t_2) \\ c_4 &= \sin(t_1) \sin(t'_1) + \cos(t_1) \cos(t'_1) \sin(t_2), \end{aligned} \quad (4)$$

demonstrating that, in general, CCSD and UCCSD amplitudes for the same state should be quite different. A general recipe for deriving the action of each term in disentangled UCC on a quantum state has been provided by Chen et al.,³³ and is shown below for single and double excitation terms:

$$\begin{aligned} \exp[\theta(\hat{a}_a^\dagger \hat{a}_i - \hat{a}_i^\dagger \hat{a}_a)] &= 1 + \sin \theta(\hat{a}_a^\dagger \hat{a}_i - \hat{a}_i^\dagger \hat{a}_a) \\ &\quad + (\cos \theta - 1)(\hat{n}_a + \hat{n}_i - 2\hat{n}_a \hat{n}_i), \end{aligned} \quad (5)$$

$$\begin{aligned} \exp[\theta(\hat{a}_{a_1}^\dagger \hat{a}_{i_1} \hat{a}_{a_2}^\dagger \hat{a}_{i_2} - \hat{a}_{i_2}^\dagger \hat{a}_{a_2} \hat{a}_{i_1}^\dagger \hat{a}_{a_1})] &= 1 + \sin \theta(\hat{a}_{a_1}^\dagger \hat{a}_{i_1} \hat{a}_{a_2}^\dagger \hat{a}_{i_2} - \hat{a}_{i_2}^\dagger \hat{a}_{a_2} \hat{a}_{i_1}^\dagger \hat{a}_{a_1}) \\ &\quad + (\cos \theta - 1)[\hat{n}_{a_1} \hat{n}_{a_2} (1 - \hat{n}_{i_1}) (1 - \hat{n}_{i_2}) \\ &\quad + (1 - \hat{n}_{a_1}) (1 - \hat{n}_{a_2}) \hat{n}_{i_1} \hat{n}_{i_2}], \end{aligned} \quad (6)$$

where θ is a cluster amplitude, i and a are, respectively, indices of orbitals occupied and unoccupied in the reference state, and $\hat{n}_\alpha = \hat{a}_\alpha^\dagger \hat{a}_\alpha$ is the number operator.

Approximate relations between pCCD and UpCCD

Motivated by the effectiveness and low cost oo-pCCD calculations, and the desire to avoid hybrid quantum-classical variational optimization or deep QRAM-type circuits, we set out to explore connections between non-unitary pCCD and trotterized UpCCD (henceafter referred to as UpCCD). Applying the small angle approximation ($\sin x \approx x, \cos x \approx 1$) to Eq. 6 and taking $i_2 = i_1 + 1, a_2 = a_1 + 1$ (paired excitations), we obtain:

$$\exp[\theta(\hat{a}_a^\dagger \hat{a}_i \hat{a}_{a+1}^\dagger \hat{a}_{i+1} - \hat{a}_{i+1}^\dagger \hat{a}_{a+1} \hat{a}_i^\dagger \hat{a}_a)] \approx 1 + \theta(\hat{a}_a^\dagger \hat{a}_i \hat{a}_{a+1}^\dagger \hat{a}_{i+1} - \hat{a}_{i+1}^\dagger \hat{a}_{a+1} \hat{a}_i^\dagger \hat{a}_a), \quad (7)$$

where we dropped the subindices for simplicity of notation. Thus, the action of each term in UpCCD can be approximated (in the limit of small amplitudes) as the sum of identity, a double excitation and a double deexcitation. To uncover the similarities between pCCD and UpCCD, we first write the pCCD wave function for 4 electrons in 4 orbitals (8 spinorbitals)

($t_{o,v}$ is the amplitude of the excitation of an electron pair from orbital o to v):

$$\begin{aligned}\Psi_{(4,4)-\text{pCCD}} = & |11110000\rangle + t_{1,2}|11001100\rangle + t_{1,3}|11000011\rangle \\ & + t_{0,2}|00111100\rangle + t_{0,3}|00110011\rangle \\ & + (t_{1,2}t_{0,3} + t_{1,3}t_{0,2})|00001111\rangle.\end{aligned}\quad (8)$$

The corresponding UpCCD wave function, assuming an operator ordering resulting from iterating first over o , then over v , can be approximated by repeated application of Eq. (7) as:

$$\begin{aligned}\Psi_{(4,4)-\text{UpCCD}} \approx & |11110000\rangle + t_{1,2}|11001100\rangle + t_{1,3}|11000011\rangle \\ & + (t_{0,2} - t_{1,2}t_{0,3}t_{1,3})|00111100\rangle + t_{0,3}|00110011\rangle \\ & + (t_{1,2}t_{0,3} + t_{1,3}t_{0,2})|00001111\rangle.\end{aligned}\quad (9)$$

We notice that Eq. 8 and 9 differ only in the coefficient of the $|00111100\rangle$ determinant, by $-t_{1,2}t_{0,3}t_{1,3}$: a term generated by two double excitations and one double deexcitation, which we call an *excitation-deexcitation term*. Being a product of three amplitudes (each being smaller than 1), this deviation from the corresponding CI coefficient in the pCCD ($= t_{0,2}$) is likely to be much smaller than the $t_{0,2}$ itself and must vanish if any of the numbers $t_{1,2}$, $t_{0,3}$ or $t_{1,3}$ is zero, rendering the small-angle-approximated UpCCD and pCCD wave functions equal, given the same amplitudes in both Ansätze. We note that the presence of excitation-deexcitation terms depends on the ordering of operators in the product formula, and e.g. reversing the operators in the above UpCCD wave function leads to this term appearing in the coefficient for $|11000011\rangle$. Furthermore, UpCCD wave functions of systems with more electrons may contain higher excitation-deexcitation terms, generated by n double excitations and $n-1$ double deexcitations, $2 \leq n \leq \frac{e_{\max}}{2}$, where e_{\max} is the highest excitation possible in the system.

Therefore, we hypothesize that pCCD and trotterized UpCCD wave functions sharing the same cluster amplitudes are approximately equal if (1) the small angle approximation is valid and (2) the coefficients of excitation-deexcitation terms vanish. The former condition is unlikely to be strictly met in practice, as at least some of the amplitudes will be large in magnitude, therefore the impact of the small-angle approximation must be verified experimentally (see below). The latter condition can be expected to hold if the matrix of cluster amplitudes is sufficiently sparse. In pCCD, compared to ‘full’ CCD, only amplitudes of paired excitations are non-zero, and we can additionally increase the sparsity by setting all amplitudes with magnitudes smaller than a chosen threshold to zero. In the following sections, we show that substituting largest oo-pCCD amplitudes into an UpCCD ansatz allows avoiding the excitation-deexcitation terms and preparation of states with high overlaps with the ground states with very shallow circuits, for a range of systems for which the Hartree-Fock wave function has low overlap with the ground state. Furthermore, we demonstrate the utility of our method in the Quantum Phase Estimation algorithm.

We note that while the small-angle approximation is as valid for UpCCD as it is for UCCD and UCCSD, it is unlikely that excitation-deexcitation terms can be small in practice for the latter UCC Ansatze, due to the vastly increased number of possibilities in which a given Slater determinant can be reached by a series of excitations and deexcitations.

Calculations

Mean-field calculations, preparation of 1- and 2-electron integrals and CASCI calculations have been performed with PySCF.³⁴ Orbital-optimized pCCD has been carried out using an in-house code (partially based on PySCF), using automatic differentiation as implemented in Jax³⁵ and the Adam³⁶ optimizer from Optax,³⁷ modified to control the step size via an adaptive trust radius, for the orbital optimization. Quantum circuits were constructed using an in-house code, build on top of pytket.³⁸ UpCCD circuits were constructed using Givens

rotation gates as described by Nam et al.,³⁰ but with an opposite sign convention for the parameters, for consistency with pCCD. Iterative and Canonical Quantum Phase Estimation simulations used a first-order product formula approximation for the evolution operator, and the eigenphase estimate was obtained from the most abundant measurement outcome. We used Qulacs³⁹ for state vector circuit simulation, and pytket-cutensornet⁴⁰ for estimation of state overlap in cases involving more than 20 qubits. Comparative experiments with CVO-QRAM¹¹ were performed with the aid of the qclib library,⁴¹ using multi-controlled gate decompositions as implemented in qiskit 2.0.0.⁴² Wherever we refer to an equivalent-fidelity CVO-QRAM circuit, we mean a circuit which prepares a state defined by as many CI determinants taken from the CASCI or HCI expansion, starting from those with largest coefficient magnitudes, as required to reach at least the same fidelity as that of the given state. Heat-bath Configuration Interaction (HCI) calculations were performed using Dice,^{8,43,44} with ϵ of $1 \times 10^{-4} - 8 \times 10^{-4}$, and 20000 largest CI coefficients were used for estimation of overlap with the UpCCD states.

Numerical results and discussion

1-D Hubbard Model

The Hubbard Hamiltonian, a widely-studied model system, is a particularly useful test bed for electronic structure methods, because its properties can be continuously tuned from non-interacting to strongly correlated.⁴⁵ While oo-pCCD does not exactly reproduce the eigenstates of 1D Hubbard chains at half-filling, it captures the static correlation effects very well, even at high values of U/t .²⁵ Therefore, we investigated the overlap of oo-pCCD-UpCCD wave functions with exact eigenstates, for half-filled 1D Hubbard models with 6 and 10 sites (corresponding to 12 and 20 qubits, respectively), varying U from 0.5t to 9t, see Fig. 1. Across the tested range of U , the UpCCD wave functions have consistently higher overlaps with the ground state than the HF states. For low values of U , the overlaps are

very high, while at high U the overlap plateaus at a value dependent on the chain length. Our state preparation circuits are very shallow: 6 and 11 gates, respectively. In contrast, for $U/t = 8$, equivalent-fidelity CVO-QRAM circuits have depths of 1144 and 54333 gates, respectively.

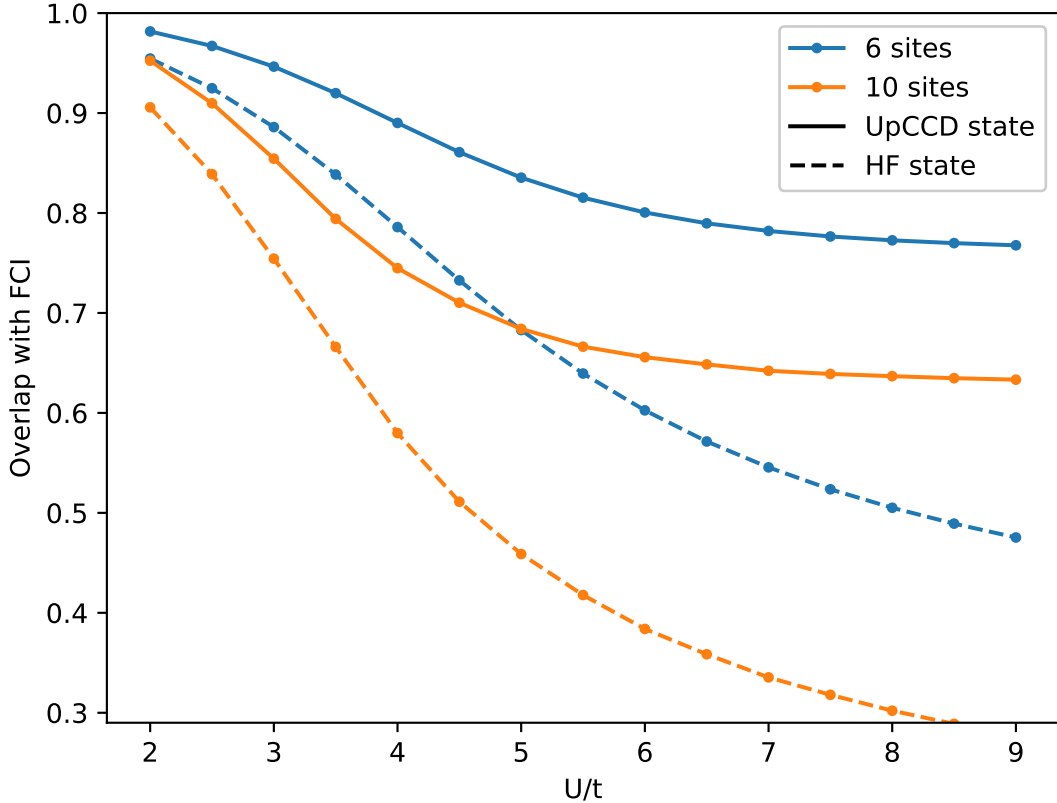


Figure 1: Overlaps of UpCCD (solid lines) and Hartree-Fock (dashed lines) states with CASCI states, for 6- and 10-site Hubbard models at half filling

Bond dissociation in ethene, ethyne and dinitrogen

Dissociation of ethene C_2H_4 into two triplet carbenes is one of the simplest reactions which require a multi-configurational wave function even for a qualitatively correct description.⁴⁶ Dissociation of dinitrogen N_2 ⁴⁷ and ethyne C_2H_2 ^{48,49} are also well-studied multi-configurational problems. For each of these systems, we varied the length of the multiple bond (and the

remaining internal coordinates, except for N_2 , were taken from the W4-11 data set⁵⁰), and performed oo-pCCD using the cc-pVDZ basis.⁵¹

Bond dissociation: 20-qubit models

For an analysis of the fidelity of our oo-pCCD-UpCCD scheme along the bond dissociation curves, we have chosen an active space of 10 electrons in 10 (spatial) orbitals: large enough to capture static correlation effects, but small enough to enable rapid calculations. For each geometry, oo-pCCD was calculated in the 10-electron, 10-orbital active space and a 20-qubit UpCCD ansatz was constructed using 4-7 pCCD amplitudes having the largest magnitudes. The ansatz was simulated using Qulacs³⁹ and the overlap with the lowest-lying singlet CASCI state (obtained for the same active space and orbitals) was computed. Fig. 2 compares the fidelities of such-constructed UpCCD states to those of Hartree-Fock (HF) states. As expected, around equilibrium geometries ($D_{CC} = 1.206 \text{ \AA}$ for C_2H_2 , $D_{CC} = 1.232 \text{ \AA}$ for C_2H_4 and $D_{NN} = 1.190 \text{ \AA}$ for N_2), both UpCCD and HF states have near-perfect overlaps with the exact ground states. However, when the multiple bonds are stretched, the quality of the HF solution deteriorates more rapidly than that of the UpCCD with pCCD amplitudes, although the behaviour is markedly different for each system. In the case of C_2H_2 , UpCCD has modest advantage over HF up to ca. 2.2-2.3 \AA (perhaps due to the avoided crossing, see Fig. 4 in Zeng et al.⁴⁹), above which the accuracy of the UpCCD ansatz improves to near-perfect, compared to 0.83-0.85 fidelity of HF. For ethene, we observe a smooth decrease of fidelity during dissociation, to about 0.84 (UpCCD) and 0.66 (HF). In the case of N_2 , HF and UpCCD have similar overlaps with CASCI up to about 1.7 \AA , where the CC ansatz starts to be superior, until ca. 2.5 \AA , above which its fidelity drops significantly. Reduction of the amplitude threshold (i.e. adding more excitations to the UpCCD ansatz) had a negligible effect on fidelities for neither of the systems. Interestingly, optimisation of the amplitudes via VQE improved the overlaps only slightly, by up to 2%.

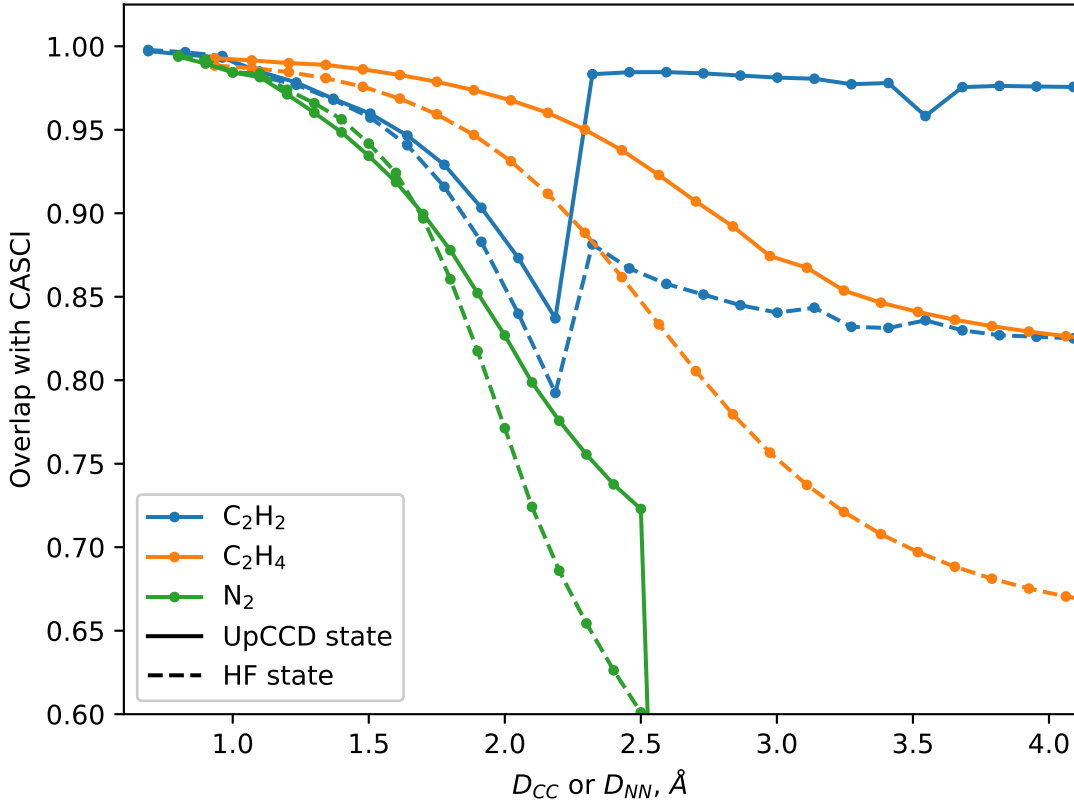


Figure 2: Overlaps of UpCCD (solid lines) and Hartree-Fock (dashed lines) states with CASCI states, for 20-qubit models of C_2H_2 , C_2H_4 and N_2 , vs. C-C or N-N distances (see text)

State fidelity in all-electron calculations

We applied the oo-pCCD-UpCCD scheme, with amplitude threshold of 0.05, to all-electron calculations of C_2H_2 at $D_{CC} = 2.38 \text{ \AA}$ (i.e. $2.0 \times D_{eq}$) and N_2 at $D_{NN} = 2.5 \text{ \AA}$ (i.e. $2.1 \times D_{eq}$), in cc-pVDZ and cc-pVTZ basis sets. Due to the number of qubits exceeding the capabilities of a state vector simulator, simulations were performed with the pytket-cutensornet tensor network simulator, and the exact ground states were approximated with Heat-Bath Configuration Interaction. The results are shown in Table 1. In each case, states prepared with very shallow circuits (depth of 7 gates) have very high (stretched ethyne) or, at least, decent, i.e. $2\times$ better than HF (stretched dinitrogen), overlaps with HCl.

For comparison, we have also constructed CVO-QRAM circuits, preparing states defined by as many highest CI coefficients as required to achieve a fidelity no smaller than that of the corresponding UpCCD state. The differences are striking: oo-pCCD-UpCCD required $2\text{--}3 \times 10^2$ lower depth than CVO-QRAM.

Table 1: Overlaps of oo-pCCD-UpCCD states with exact ground states of stretched C_2H_2 and N_2 molecules

System	Basis	N_q	$\langle \Phi_{\text{UpCCD}} \Phi_{\text{HCl}} \rangle$	Depth	$\langle \Phi_{\text{HF}} \Phi_{\text{HCl}} \rangle$	CVO-QRAM depth
C_2H_2	cc-pVDZ	76	0.95	7	0.76	1320
C_2H_2	cc-pVTZ	176	0.95	7	0.76	
N_2	cc-pVDZ	56	0.69	7	0.34	2335
N_2	cc-pVTZ	120	0.69	7	0.34	

To shed more light on why UpCCD with leading oo-pCDD amplitudes approximates these ground states so well, we first derive the small-angle-approximated formula for the stretched C_2H_2 in cc-pVDZ basis, where, with the amplitude threshold of 0.1 we have only three amplitudes: $t_{2,8} = -0.1575$; $t_{5,9} = -0.1569$; $t_{6,7} = -0.7315$. We notice that the resultant formula contains no excitation-deexcitation terms and is equal to the pCCD formula (trailing zeros in kets have been omitted for clarity):

$$\begin{aligned}
\Psi_{\text{UpCCD}(\text{C}_2\text{H}_2)} \approx & \Psi_{\text{sa-UpCCD}(\text{C}_2\text{H}_2)} |1111111111111000000... \rangle \\
& + t_{6,7} |1111111111100110000... \rangle \\
& + t_{5,9} |1111111110011000011... \rangle \\
& + t_{5,9} t_{6,7} |1111111110000110011... \rangle \\
& + t_{2,8} |1111001111111001100... \rangle \\
& + t_{2,8} t_{6,7} |11110011111100111100... \rangle \\
& + t_{2,8} t_{5,9} |11110011110011001111... \rangle \\
& + t_{2,8} t_{5,9} t_{6,7} |11110011110000111111... \rangle \\
= & \Psi_{\text{pCCD}(\text{C}_2\text{H}_2)}. \tag{10}
\end{aligned}$$

We can now assess the impact of the small-angle approximation by comparing the above wave function with the CI coefficients computed with the exact UpCCD formula (obtained by application of Eq. (6), and with the CI coefficients from the HCI state, see Table 2 (note that both UpCCD and pCCD states comprised only the largest 3 amplitudes). Even though the magnitudes of the amplitudes are too large for the small-angle approximation to be very accurate, the overlap between pCCD and UpCCD wave functions is nearly perfect, and both CC wave functions have very similar and high overlaps with HCI. Notably, their overlaps with HCI are only slightly lower than the overlap between HCI and its seniority-zero sector (0.9751).

Table 2: Comparison of corresponding CI coefficients of normalized pCCD, UpCCD and HCI states of stretched C_2H_2 , $D_{CC} = 2.38$ (Å), cc-pVDZ basis (36 orbitals)

Determinant	pCCD	UpCCD	HCI
$ \text{111111111111000000...}\rangle$	0.7071	0.7259	0.7553
$ \text{11111111111100110000...}\rangle$	-0.6612	-0.6516	-0.5451
$ \text{11111111110011000011...}\rangle$	-0.1419	-0.1149	-0.1343
$ \text{11111111110000110011...}\rangle$	0.1038	0.1031	0.0943
$ \text{1111001111111001100...}\rangle$	-0.1424	-0.1153	-0.1350
$ \text{11110011111100111100...}\rangle$	0.1042	0.1035	0.0948
$ \text{11110011110011001111...}\rangle$	0.0224	0.0182	0.0213
$ \text{11110011110000111111...}\rangle$	-0.0164	-0.0164	-0.0148
Overlap with pCCD	1	0.9990	0.9531
Overlap with HCI	0.9531	0.9546	1

An analogous analysis for the stretched N_2 system leads to similar conclusions: despite three amplitudes being large ($t_{3,9} = -0.02566$; $t_{4,9} = -0.6073$; $t_{5,7} = -0.8787$; $t_{6,8} = -0.8787$), the overlap between pCCD and UpCCD states is high and both states are approximately equally close to the HCI ground state, see Table 3 (note that both UpCCD and pCCD states comprised only the largest 4 amplitudes). Interestingly, the overlap of pCCD with HCI is almost exactly equal to the overlap of the seniority-zero sector of HCI with HCI (0.7170).

Table 3: Comparison of corresponding CI coefficients of normalized pCCD, UpCCD and HCI states of stretched N_2 , $D_{NN} = 3.5$ (Å), cc-pVDZ basis (56 orbitals)

Determinant	pCCD	UpCCD	HCI
$ \text{11111111111111000000...}\rangle$	0.4823	0.3344	0.3463
$ \text{11111111111100001100...}\rangle$	-0.4238	-0.4034	-0.2998
$ \text{11111111110011110000...}\rangle$	-0.4238	-0.4034	-0.2998
$ \text{11111111110000111100...}\rangle$	0.3724	0.4867	0.2625
$ \text{11111111100001111000...}\rangle$	-0.2929	-0.2324	-0.2073
$ \text{111111110011110000111...}\rangle$	0.2574	0.2804	0.1883
$ \text{11111111000011110011...}\rangle$	0.2574	0.2804	0.1883
$ \text{11111111000000111111...}\rangle$	-0.2261	-0.3383	-0.1734
$ \text{11111100111111000011...}\rangle$	-0.0061	-0.0042	-0.0098
$ \text{11111100111100001111...}\rangle$	0.0054	0.0051	0.008
$ \text{11111100110011110011...}\rangle$	0.0054	0.0051	0.008
$ \text{11111100110000111111...}\rangle$	-0.0047	-0.0062	-0.0066
Overlap with pCCD	1	0.9734	0.7159
Overlap with HCI	0.7159	0.6980	1

Application to Quantum Phase Estimation

To demonstrate the usefulness of the oo-pCCD-UpCCD scheme for state preparation for QPE, we have revisited the ethene dissociation reaction mentioned above. We constructed a minimal model of the double bond dissociation in C_2H_4 , using (4,4)-CASSCF orbitals in cc-pVDZ basis, at the geometry as reported in the W4-11 data set,⁵⁰ set the C-C distance to 3.23 Å (i.e. $D_{eq} + 2$ Å). Note that the lowest singlet state at this geometry corresponds to two coupled triplet carbenes.⁴⁶ We performed oo-pCCD, restricting the orbital rotation to the active space. Plugging the two largest pCCD amplitudes into UpCCD, we obtain $\langle \Psi_{UpCCD} | \Psi_{CASSCF} \rangle = 0.83$ (cf. $\langle \Psi_{HF} | \Psi_{CASSCF} \rangle = 0.67$). We then perform Canonical Quantum Phase Estimation (with up to 12 ancilla registers) and Iterative Quantum Phase Estimation (with k up to 14),¹ using the UpCCD or HF states as the initial states, see Fig. 3. Clearly, the HF state is insufficiently close to the ground state to ensure success, while (I)QPE applied to the UpCCD initial state converges to the ground state energy.

The impact of state preparation method is even more evident when we plot the histogram of energies obtained from 12-ancilla canonical QPE sampled 1000 times (Fig. 4): initializa-

tion with UpCCD yields a large peak corresponding to the ground state and 2-3 smaller peaks of excited states, while starting from the HF state results in a complicated spectrum, in which the ground state peak is relatively small and requires many measurements to resolve.

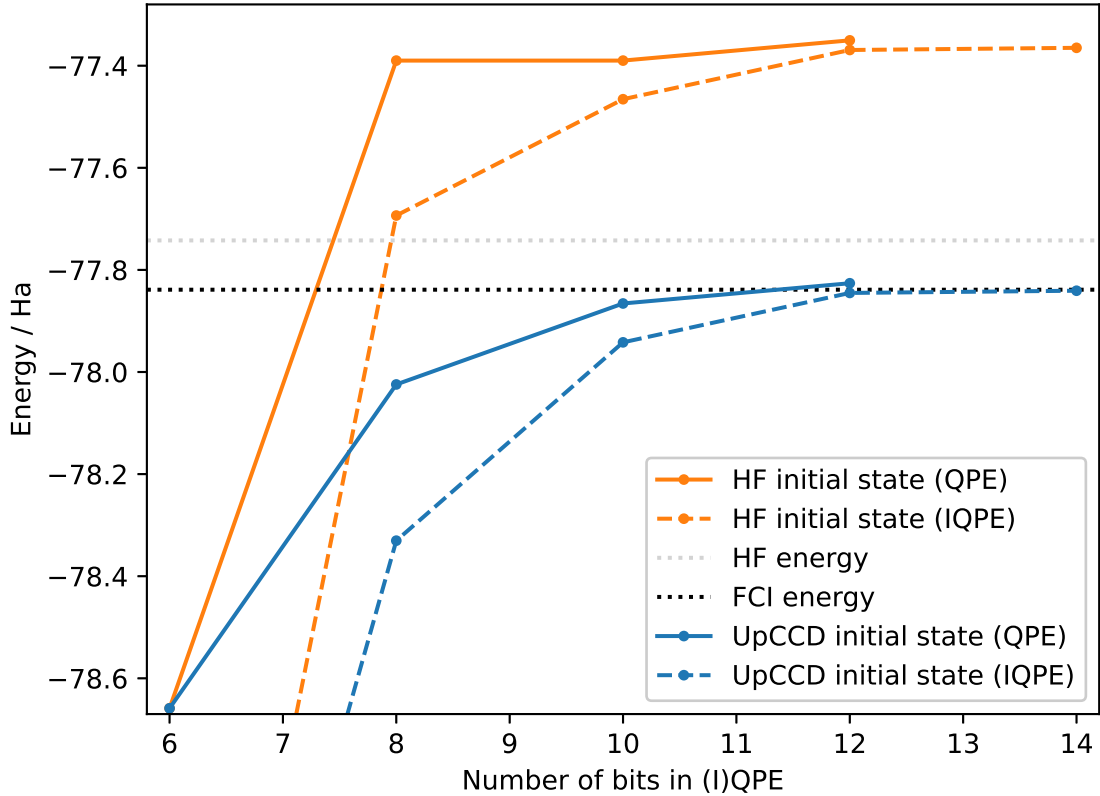


Figure 3: Effect of the initial state on the outcome of Canonical and Iterative Quantum Phase Estimation applied to singlet state of dissociated C_2H_4

Conclusions and Outlook

In this work, we have derived the connection between oo-pCCD and UpCCD wave functions in the small-amplitude limit, and introduced the oo-pCCD-UpCCD ansatz as a non-variational approximate state preparation method for singlet states, for use with Quantum Phase Estimation. We evaluated the effectiveness of our scheme in preparing high-fidelity states, on prototypical multi-configurational examples of double bond dissociation (ethene)

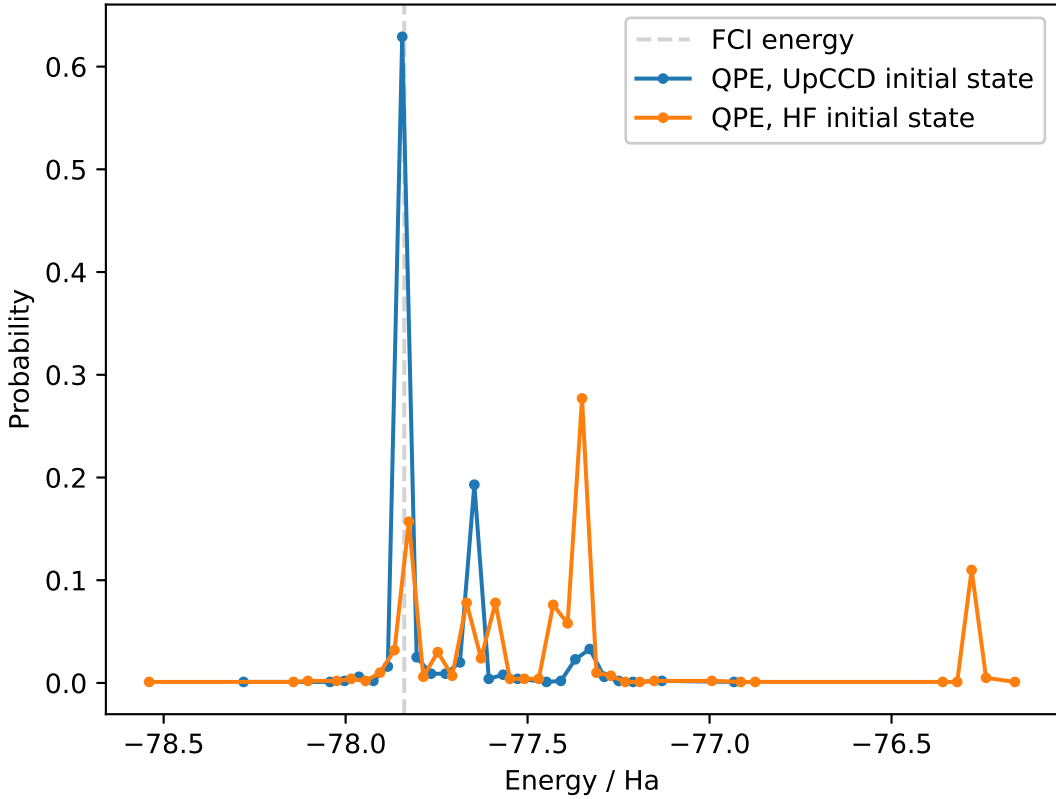


Figure 4: Effect of the initial state on the outcome of Canonical Quantum Phase Estimation applied to singlet state of dissociated C_2H_4 : histogram of energies (1000 samples)

and triple bond dissociation (ethyne and dinitrogen), as well as on a model Hamiltonian with correlation tunable from weak to strong (1D Hubbard models with 6 and 10 sites). In each case, the UpCCD ansatz circuits with leading oo-pCCD amplitudes were embarrassingly shallow and prepared states with significantly higher fidelities than the Hartree-Fock state (apart from N_2 with $D_{NN} < 1.6$, where overlaps of UpCCD and HF with HCl were similar and > 0.9); high enough to ensure success of Quantum Phase Estimation. We show, on the stretched C_2H_2 and N_2 examples, that the pCCD state has almost unit overlap with the seniority-zero sector of HCl, and that the overlap between pCCD and UpCCD states is high, owing to the sparsity of the amplitude matrix ensuring lack of excitation-deexcitation terms and limited impact of the error due to the small-angle approximation. Finally, we demon-

strate how our scheme enables successful estimation of ground state energy of an 8-qubit model of dissociated ethene.

Overall, this study enhances our understanding of the connections between non-unitary and unitary coupled cluster methods with paired doubles, and provides a low cost method for preparing high-fidelity singlet states, for use with QPE and related methods.

References

- (1) Kitaev, A. Y. Quantum measurements and the Abelian stabilizer problem. *arXiv preprint quant-ph/9511026* **1995**,
- (2) Abrams, D. S.; Lloyd, S. Quantum algorithm providing exponential speed increase for finding eigenvalues and eigenvectors. *Physical Review Letters* **1999**, *83*, 5162.
- (3) Lee, S. et al. Evaluating the evidence for exponential quantum advantage in ground-state quantum chemistry. *Nature communications* **2023**, *14*, 1952.
- (4) Tubman, N. M.; Mejuto-Zaera, C.; Epstein, J. M.; Hait, D.; Levine, D. S.; Huggins, W.; Jiang, Z.; McClean, J. R.; Babbush, R.; Head-Gordon, M.; others Postponing the orthogonality catastrophe: efficient state preparation for electronic structure simulations on quantum devices. *arXiv preprint arXiv:1809.05523* **2018**,
- (5) Feniou, C.; Adjoua, O.; Claudon, B.; Zylberman, J.; Giner, E.; Piquemal, J.-P. Sparse quantum state preparation for strongly correlated systems. *The Journal of Physical Chemistry Letters* **2024**, *15*, 3197–3205.
- (6) Fomichev, S.; Hejazi, K.; Zini, M. S.; Kiser, M.; Fraxanet, J.; Casares, P. A. M.; Delgado, A.; Huh, J.; Voigt, A.-C.; Mueller, J. E.; others Initial state preparation for quantum chemistry on quantum computers. *PRX Quantum* **2024**, *5*, 040339.

(7) Tubman, N. M.; Lee, J.; Takeshita, T. Y.; Head-Gordon, M.; Whaley, K. B. A deterministic alternative to the full configuration interaction quantum Monte Carlo method. *The Journal of chemical physics* **2016**, *145*.

(8) Sharma, S.; Holmes, A. A.; Jeanmairet, G.; Alavi, A.; Umrigar, C. J. Semistochastic heat-bath configuration interaction method: Selected configuration interaction with semistochastic perturbation theory. *Journal of chemical theory and computation* **2017**, *13*, 1595–1604.

(9) Huron, B.; Malrieu, J.; Rancurel, P. Iterative perturbation calculations of ground and excited state energies from multiconfigurational zeroth-order wavefunctions. *The Journal of Chemical Physics* **1973**, *58*, 5745–5759.

(10) Babbush, R.; Gidney, C.; Berry, D. W.; Wiebe, N.; McClean, J.; Paler, A.; Fowler, A.; Neven, H. Encoding electronic spectra in quantum circuits with linear T complexity. *Physical Review X* **2018**, *8*, 041015.

(11) de Veras, T. M.; da Silva, L. D.; da Silva, A. J. Double sparse quantum state preparation. *Quantum Information Processing* **2022**, *21*, 204.

(12) Berry, D. W.; Tong, Y.; Khattar, T.; White, A.; Kim, T. I.; Low, G. H.; Boixo, S.; Ding, Z.; Lin, L.; Lee, S.; others Rapid Initial-State Preparation for the Quantum Simulation of Strongly Correlated Molecules. *PRX Quantum* **2025**, *6*, 020327.

(13) Chan, G. K.-L.; Sharma, S. The density matrix renormalization group in quantum chemistry. *Annual review of physical chemistry* **2011**, *62*, 465–481.

(14) Schön, C.; Solano, E.; Verstraete, F.; Cirac, J. I.; Wolf, M. M. Sequential generation of entangled multiqubit states. *Physical review letters* **2005**, *95*, 110503.

(15) Peruzzo, A.; McClean, J.; Shadbolt, P.; Yung, M.-H.; Zhou, X.-Q.; Love, P. J.; Aspuru-

Guzik, A.; O'brien, J. L. A variational eigenvalue solver on a photonic quantum processor. *Nature communications* **2014**, *5*, 4213.

(16) Gard, B. T.; Zhu, L.; Barron, G. S.; Mayhall, N. J.; Economou, S. E.; Barnes, E. Efficient symmetry-preserving state preparation circuits for the variational quantum eigensolver algorithm. *npj Quantum Information* **2020**, *6*, 10.

(17) Larocca, M.; Thanasilp, S.; Wang, S.; Sharma, K.; Biamonte, J.; Coles, P. J.; Cincio, L.; McClean, J. R.; Holmes, Z.; Cerezo, M. A review of barren plateaus in variational quantum computing. *arXiv preprint arXiv:2405.00781* **2024**,

(18) Astrakhantsev, N.; Mazzola, G.; Tavernelli, I.; Carleo, G. Phenomenological theory of variational quantum ground-state preparation. *Physical Review Research* **2023**, *5*, 033225.

(19) Gonthier, J. F.; Radin, M. D.; Buda, C.; Doskocil, E. J.; Abuan, C. M.; Romero, J. Measurements as a roadblock to near-term practical quantum advantage in chemistry: Resource analysis. *Physical Review Research* **2022**, *4*, 033154.

(20) Limacher, P. A.; Ayers, P. W.; Johnson, P. A.; De Baerdemacker, S.; Van Neck, D.; Bultinck, P. A new mean-field method suitable for strongly correlated electrons: Computationally facile antisymmetric products of nonorthogonal geminals. *Journal of chemical theory and computation* **2013**, *9*, 1394–1401.

(21) Bytautas, L.; Henderson, T. M.; Jiménez-Hoyos, C. A.; Ellis, J. K.; Scuseria, G. E. Seniority and orbital symmetry as tools for establishing a full configuration interaction hierarchy. *The Journal of chemical physics* **2011**, *135*.

(22) Kossoski, F.; Damour, Y.; Loos, P.-F. Hierarchy configuration interaction: Combining seniority number and excitation degree. *The journal of physical chemistry letters* **2022**, *13*, 4342–4349.

(23) Couty, M.; Hall, M. B. Generalized molecular orbital theory II. *The Journal of Physical Chemistry A* **1997**, *101*, 6936–6944.

(24) Henderson, T. M.; Bulik, I. W.; Stein, T.; Scuseria, G. E. Seniority-based coupled cluster theory. *The Journal of chemical physics* **2014**, *141*.

(25) Stein, T.; Henderson, T. M.; Scuseria, G. E. Seniority zero pair coupled cluster doubles theory. *The Journal of chemical physics* **2014**, *140*.

(26) Shepherd, J. J.; Henderson, T. M.; Scuseria, G. E. Using full configuration interaction quantum Monte Carlo in a seniority zero space to investigate the correlation energy equivalence of pair coupled cluster doubles and doubly occupied configuration interaction. *The Journal of Chemical Physics* **2016**, *144*.

(27) Anand, A.; Schleich, P.; Alperin-Lea, S.; Jensen, P. W.; Sim, S.; Díaz-Tinoco, M.; Kottmann, J. S.; Degroote, M.; Izmaylov, A. F.; Aspuru-Guzik, A. A quantum computing view on unitary coupled cluster theory. *Chemical Society Reviews* **2022**, *51*, 1659–1684.

(28) Elfving, V. E.; Gámez, J. A.; Gogolin, C. Efficient quantum chemistry simulation using gate-based qubit quantum devices. 'WO 2021/099428 A1', 2021.

(29) Elfving, V. E.; Millaruelo, M.; Gámez, J. A.; Gogolin, C. Simulating quantum chemistry in the seniority-zero space on qubit-based quantum computers. *Physical Review A* **2021**, *103*, 032605.

(30) Nam, Y.; Chen, J.-S.; Pisenti, N. C.; Wright, K.; Delaney, C.; Maslov, D.; Brown, K. R.; Allen, S.; Amini, J. M.; Apisdorf, J.; others Ground-state energy estimation of the water molecule on a trapped-ion quantum computer. *npj Quantum Information* **2020**, *6*, 33.

(31) Cowtan, A.; Simmons, W.; Duncan, R. A generic compilation strategy for the unitary coupled cluster ansatz. *arXiv preprint arXiv:2007.10515* **2020**,

(32) Evangelista, F. A.; Chan, G. K.; Scuseria, G. E. Exact parameterization of fermionic wave functions via unitary coupled cluster theory. *The Journal of chemical physics* **2019**, *151*.

(33) Chen, J.; Cheng, H.-P.; Freericks, J. K. Quantum-inspired algorithm for the factorized form of unitary coupled cluster theory. *Journal of Chemical Theory and Computation* **2021**, *17*, 841–847.

(34) Sun, Q.; Zhang, X.; Banerjee, S.; Bao, P.; Barbry, M.; Blunt, N. S.; Bogdanov, N. A.; Booth, G. H.; Chen, J.; Cui, Z.-H.; others Recent developments in the PySCF program package. *The Journal of chemical physics* **2020**, *153*.

(35) Bradbury, J.; Frostig, R.; Hawkins, P.; Johnson, M. J.; Leary, C.; Maclaurin, D.; Necula, G.; Paszke, A.; VanderPlas, J.; Wanderman-Milne, S.; Zhang, Q. JAX: composable transformations of Python+NumPy programs. 2025; <http://github.com/jax-ml/jax>.

(36) Kingma, D. P. Adam: A method for stochastic optimization. *arXiv preprint arXiv:1412.6980* **2014**,

(37) DeepMind et al. The DeepMind JAX Ecosystem. 2025; <http://github.com/google-deepmind>.

(38) Sivarajah, S.; Dilkes, S.; Cowtan, A.; Simmons, W.; Edgington, A.; Duncan, R. "t|ket>: a retargetable compiler for NISQ devices". *Quantum Science and Technology* **2020**, *6*, 014003.

(39) Suzuki, Y.; Kawase, Y.; Masumura, Y.; Hiraga, Y.; Nakadai, M.; Chen, J.; Nakanishi, K. M.; Mitarai, K.; Imai, R.; Tamiya, S.; others Qulacs: a fast and versatile quantum circuit simulator for research purpose. *Quantum* **2021**, *5*, 559.

(40) Quantinuum pytket-cutensornet. 2025; <https://github.com/CQCL/pytket-cutensornet>.

(41) Araujo, I. F.; Araújo, I. C. S.; da Silva, L. D.; Blank, C.; da Silva, A. J. Quantum computing library. 2025; <https://github.com/qclib/qclib>.

(42) Javadi-Abhari, A.; Treinish, M.; Krsulich, K.; Wood, C. J.; Lishman, J.; Gacon, J.; Martiel, S.; Nation, P. D.; Bishop, L. S.; Cross, A. W.; Johnson, B. R.; Gambetta, J. M. Quantum computing with Qiskit. 2024.

(43) Holmes, A. A.; Tubman, N. M.; Umrigar, C. Heat-bath configuration interaction: An efficient selected configuration interaction algorithm inspired by heat-bath sampling. *Journal of chemical theory and computation* **2016**, *12*, 3674–3680.

(44) Smith, J. E.; Mussard, B.; Holmes, A. A.; Sharma, S. Cheap and near exact CASSCF with large active spaces. *Journal of chemical theory and computation* **2017**, *13*, 5468–5478.

(45) Scalettar, R. T. An introduction to the Hubbard Hamiltonian. *Quantum materials: experiments and theory* **2016**, *6*.

(46) Ohta, K.; Davidson, E. R.; Morokuma, K. Dimerization paths of CH₂ and SiH₂ fragments to ethylene, disilene, and silaethylene: MCSCF and MRCI study of least-and non-least-motion paths. *Journal of the American Chemical Society* **1985**, *107*, 3466–3471.

(47) Chan, G. K.-L.; Kállay, M.; Gauss, J. State-of-the-art density matrix renormalization group and coupled cluster theory studies of the nitrogen binding curve. *The Journal of Chemical Physics* **2004**, *121*, 6110–6116.

(48) Siegbahn, P. E. M. Large scale contracted MC–CI calculations on acetylene and its

dissociation into two CH(2Π) radicals. *The Journal of Chemical Physics* **1981**, *75*, 2314–2320.

(49) Zeng, T.; Wang, H.; Lu, Y.; Xie, Y.; Wang, H.; Schaefer III, H. F.; Ananth, N.; Hoffmann, R. Tuning spin-states of carbynes and silylynes: A long jump with one leg. *Journal of the American Chemical Society* **2014**, *136*, 13388–13398.

(50) Karton, A.; Daon, S.; Martin, J. M. W4-11: A high-confidence benchmark dataset for computational thermochemistry derived from first-principles W4 data. *Chemical Physics Letters* **2011**, *510*, 165–178.

(51) Dunning, T. H. Gaussian basis sets for use in correlated molecular calculations. I. The atoms boron through neon and hydrogen. *The Journal of Chemical Physics* **1989**, *90*, 1007–1023.

TOC Graphic

